Optimal Elevation of -Cell 11-Hydroxysteroid Dehydrogenase Type 1 Is a Compensatory Mechanism That Prevents High-Fat Diet–Induced -Cell Failure

Optimal Elevation of β-Cell 11β-Hydroxysteroid Dehydrogenase Type 1 Is a Compensatory Mechanism That Prevents High-Fat Diet–Induced β-Cell Failure

Sophie Turban,[1] Xiaoxia Liu,[1] Lynne Ramage,[1] Scott P. Webster,[2] Brian R. Walker,[2] Donald R. Dunbar,[3] John J. Mullins,[4] Jonathan R. Seckl,[2] and Nicholas M. Morton[1]

Type 2 diabetes ultimately results from pancreatic β-cell failure. Abnormally elevated intracellular regeneration of glucocorticoids by the enzyme 11β-hydroxysteroid dehydrogenase type 1 (11β-HSD1) in fat or liver may underlie pathophysiological aspects of the metabolic syndrome. Elevated 11β-HSD1 is also found in pancreatic islets of obese/diabetic rodents and is hypothesized to suppress insulin secretion and promote diabetes. To define the direct impact of elevated pancreatic β-cell 11β-HSD1 on insulin secretion, we generated β-cell–specific, 11β-HSD1–overexpressing (MIP-HSD1) mice on a strain background prone to β-cell failure. Unexpectedly, MIP-HSD1$^{tg/+}$ mice exhibited a reversal of high fat–induced β-cell failure through augmentation of the number and intrinsic function of small islets in association with induction of heat shock, protein kinase A, and extracellular signal–related kinase and p21 signaling pathways. 11β-HSD1$^{-/-}$ mice showed mild β-cell impairment that was offset by improved glucose tolerance. The benefit of higher β-cell 11β-HSD1 exhibited a threshold because homozygous MIP-HSD1$^{tg/tg}$ mice and diabetic Lep$^{db/db}$ mice with markedly elevated β-cell 11β-HSD1 levels had impaired basal β-cell function. Optimal elevation of β-cell 11β-HSD1 represents a novel biological mechanism supporting compensatory insulin hypersecretion rather than exacerbating metabolic disease. These findings have immediate significance for current therapeutic strategies for type 2 diabetes. ***Diabetes* 61:642–652, 2012**

Type 2 diabetes prevalence has risen dramatically in parallel with the worldwide increase in obesity (1). Understanding and targeting the processes leading to β-cell exhaustion in the face of peripheral insulin resistance is therefore of major importance. Glucocorticoid hormones potently regulate metabolism and, in rare cases of excess (Cushing syndrome), cause metabolic syndrome (2). Elevated local tissue glucocorticoid excess, driven by increased levels of the intracellular glucocorticoid regenerating enzyme 11β-hydroxysteroid dehydrogenase type 1 (11β-HSD1), particularly in adipose tissue, is implicated in the development of idiopathic metabolic syndrome (3). This premise is strongly supported by the phenotype of transgenic mice overexpressing 11β-HSD1 in fat or liver, which recapitulates diabetes and insulin-resistant metabolic disease, and by the protection from metabolic disease exhibited by 11β-HSD1$^{-/-}$ mice (3).

11β-HSD1 is also found in pancreatic islets (4). 11β-HSD1 is elevated in islets of diabetic rodents (4–6), where it was hypothesized to promote β-cell failure by amplifying the suppressive effects of glucocorticoids on insulin secretion (7,8). Although this strengthens the growing contention that 11β-HSD1 inhibitors are an effective therapeutic treatment for metabolic syndrome through actions in multiple organ systems (9), any physiological role of β-cell 11β-HSD1, and indeed the potentially pathogenic role (5–8) of elevated 11β-HSD1 in islets in vivo, remains uncertain. To test the hypothesis that increased β-cell 11β-HSD1 is diabetogenic, we used the insulin-I promoter (10) to drive β-cell–specific 11β-HSD1 elevation in vivo in C57Bl/KsJ mice, a strain prone to high-fat (HF) diet–induced β-cell failure (11).

RESEARCH DESIGN AND METHODS

Animals. All experiments conformed to local ethical guidelines and the Home Office (U.K.) Animals Scientific Procedures Act (1986). Male C57BL/KsJ, C57BL/6J (The Jackson Laboratory, Bar Harbor, ME), BKS.Cg+Leprdb/+Leprdb/OlaHsd (Lep$^{db/db}$) (Harlan, Bicester, U.K.), and inbred C57BL/6J-11β-HSD1$^{-/-}$ mice were housed as previously described (12). Mice were fed an HF diet (D12331; Research Diets, New Brunswick, NJ) or control diet (CD) (D12328) for 12 weeks from 4 weeks of age.

Generation of MIP-rHSD1 transgenic mice. An 8.3-kb (*Hin*dIII [−8280]/*Not*I [+12]) fragment of the mouse insulin gene promoter I (MIP) (gift of Mark Magnusson, Vanderbilt University, Nashville, TN) (10) and the 1.265-bp *Eco*RI fragment of the rat 11β-HSD1 (rHSD1) were cloned into pGEM11Zf(+) to create the MIP-rHSD1 transgene. The MIP-rHSD1 (10.2 kb) transgene was removed with *Hin*dIII/*Sfi*I and microinjected into the pronuclei of fertilized oocytes from C57BL/KsJ mice by standard techniques (Genetic Intervention and Screening Technologies, University of Edinburgh). The transgene was detected by PCR on tail genomic DNA using primer sequences: MIP-rHSD1, 5′-GGAACTGTGAAACAGTCCAAGG-3′ and 5′-TTTGCTGGCCCCAGTGACAAGCTTT-3′; HSD1, 5′-AAAGCTTGTCACTGGGGCCAGCAAA-3′ and 5′-AGGATCCAGAGCAAACTTGCTTGCA-3′; and glyceraldehyde-3-phosphate dehydrogenase (GAPDH), 5′GCCAAGGTCATCCATGACAAC and 5′-AGTGTAGCCCAAGATGCCCTT-3′. The mice were genotyped by Southern blotting analysis of genomic DNA using *Afl*III digestion and $^{[\alpha\text{-}32P]}$*d*-CTP–labeled rHSD1 cDNA. Transgenic heterozygotes MIP-HSD1$^{tg/+}$ were maintained on the C57BL/KsJ genetic background, and littermate wild-type C57BL/KsJ mice were used as controls.

Transgene expression. 11β-HSD1 activity was tested in rat INS1E cells (a gift of C. Wollheim, University of Geneva, Geneva, Switzerland) and mouse MIN6 cells (a gift of G. Rutter, Imperial College London, London, U.K.) 48 h after MIP-rHSD1 lipofection (Invitrogen, Paisley, U.K.).

Islet isolation and preparation. Pancreata were digested with collagenase XI (Sigma-Aldrich, Dorset, U.K.), and islets were hand-picked under a

From the [1]Molecular Metabolism Group, University of Edinburgh/British Heart Foundation Centre for Cardiovascular Science, Queen's Medical Research Institute, University of Edinburgh, Edinburgh, U.K.; the [2]Endocrinology Unit, University of Edinburgh/British Heart Foundation Centre for Cardiovascular Science, Queen's Medical Research Institute, University of Edinburgh, Edinburgh, U.K.; the [3]Bioinformatics Core, University of Edinburgh/British Heart Foundation Centre for Cardiovascular Science, Queen's Medical Research Institute, University of Edinburgh, Edinburgh, U.K.; and [4]Molecular Physiology, University of Edinburgh/British Heart Foundation Centre for Cardiovascular Science, Queen's Medical Research Institute, University of Edinburgh, Edinburgh, U.K.

Corresponding author: Nicholas M. Morton, nik.morton@ed.ac.uk.

Received 28 July 2011 and accepted 5 December 2011.

DOI: 10.2337/db11-1054

This article contains Supplementary Data online at http://diabetes.diabetesjournals.org/lookup/suppl/doi:10.2337/db11-1054/-/DC1.

stereomicroscope in Hanks' balanced salt solution and 10% FBS (Lonza, Berkshire, U.K.). For 11β-HSD1 activity assay (13), batches of 100 islets/cell lines were incubated in RPMI 1640 medium, 10% FBS, and 2.8, 16.8, or 5.5 mmol/L glucose for 24 h. For RNA extraction, islets were directly homogenized in TRIzol reagent (Life Technologies, Paisley, U.K.). For insulin secretion studies, batches of 10 islets were allowed to rest (2 h) in basal Krebs (1% weight for volume [w/v] BSA fraction V, 2.8 mmol/L glucose) on 8-μm inserts (Millipore, Billerica, MA) suspended in 12-well culture dishes. Samples were collected every 5 or 10 min for discrimination of the basal and glucose-stimulated (16.8 mmol/L glucose) insulin secretion (GSIS). A return to 2.8 mmol/L verified specificity of the response. For membrane-proximal secretion analysis, islets were preincubated (2 h) with 0.5 μg/ml brefeldin A (BFA) and 15 μmol/L cycloheximide (CHX) (Applichem, Darmstadt, Germany) and then incubated for 30 min in basal Krebs. For potassium-stimulated insulin secretion (PSIS), islets were preincubated (2 h) in basal Krebs for 30 min and then for 30 min with 40 mmol/L KCl. Acute (2 h) steroid effects (20 or 200 nmol/L 11-dehydrocorticosterone [11-DHC]) were investigated using Krebs and the 11β-HSD1 inhibitor UE2316 (1 μmol/L) or the glucocorticoid receptor (GR) antagonist RU486 (1 μmol/L). Fatty acid effects were investigated using RPMI 1640 medium, 5.5 mmol/L glucose, 10% FBS, 1% BSA, 20 nmol 11-DHC, with or without 0.5 mmol/L palmitate (22 h) followed by equilibration in Krebs (2 h) and then 2.8 mmol/L (30 min) and 16.8 mmol/L (30 min) incubations. Insulin was measured by radioimmunoassay (Linco Research, St. Charles, MO).

RNA extraction and gene expression analysis. Isolated islet total RNA was purified using PureLink RNA micro kit (Invitrogen, Paisley, U.K.). Random-primed cDNA was synthesized using Superscript III reverse transcriptase (Invitrogen). For real-time PCR, cDNA was mixed with light cycler 480 probes master mix (Roche Diagnostics, Indianapolis, IN) and probes of interest: mouse β-actin, 4352933E; Cdkn1a, Mm00432448_1; Prkacb, Mm00440840_1; Braf, Mm01165837_1; Hspa1b, Mm03038954_s1; HSD11b1, Mm00476182-m1; TBP, Mm00446973-m1 (Applied Biosystems, Warrington, U.K.).

Microarray analysis. Total islet RNA was processed through standard Affymetrix Mouse Genome 430-2.0 GeneChip protocols (ARK Genomics, Roslin Institute, Edinburgh, U.K.). Data were extracted through the GCOS software, and CEL files were imported into Bioconductor, normalized by RMA in the Affy module, and statistically analyzed with the Limma and Rank products (RankProd) packages. Gene ontology and Kyoto Encyclopedia of Genes and Genomes pathway enrichment analysis was done with the DAVID tool. Data are available in the Gene Expression Omnibus database (http://www.ncbi.nlm.nih.gov/geo/) under accession number GSE23161.

Intravenous glucose tolerance test. Mice were anesthetized by intraperitoneal injection of 1 mg/mL medetomidine (Domitor) and 100 mg/mL ketamine (Vetalar) (0.1 mL/10 g body weight). The right jugular vein was cannulated with microrenathane tubing (0.25 inch outer diameter × 0.012 inch inner diameter; Sandown Scientific, Hampton, U.K.). The cannula was exteriorized on the back of the neck and mice were allowed to recover for 2 days. Mice were fasted for 4 h before saline (0.2 μl/min, 2 h) and then glucose (25% w/v) was infused (10 μl/min/30 g body weight) into the mice (CMA/102 microdialysis pump; CMA Microdialysis, Solna, Sweden). Glucose infusion was stopped at 60 min. At 0, 1, 3, 5, 10, 15, 30, 60, and 120 min, blood glucose was measured using a OneTouch Ultra (Johnson and Johnson, Bucks, U.K.). Insulin was measured by ELISA (CrystalChem, Chicago, IL).

Intraperitoneal glucose tolerance test. Mice were fasted for 6 h and then injected intraperitoneally with 2 mg/g body wt. D-glucose (25% v/w). Blood was sampled at 0, 2, 5, 10, 15, 30, 60, and 120-min intervals after glucose bolus. Blood glucose was determined using Infinity reagent (Thermotrace, Leeds, U.K.) and insulin by ELISA (CrystalChem).

Blood corticosterone level. Singly housed mice were sampled by venesection at 8:00 A.M. within 1 min of cage disturbance. Plasma corticosterone levels were measured by radioimmunoassay as previously described (12).

Plasma triglyceride and nonesterified fatty acid levels. Triglyceride (Infinity; Thermo Fisher Scientific, Middletown, VA) and nonesterified fatty acid (NEFA) (Wako, Richmond, VA) were measured in plasma of fed or 6-h fasted mice after tail venesection.

Western blotting. Batches of 60 islets were incubated in RPMI 1640 medium (11.1 mmol/L glucose) and 10% FBS for 24 h with or without 1 μmol/L UE2316 11β-HSD1 inhibitor or 5 μmol/L KT5720 cAMP-dependent protein kinase (PKA) phosphorylation inhibitor (Sigma-Aldrich). Islets were homogenized in lysis buffer (50 mmol/L Tris, pH 7.4, 0.27 mol/L sucrose, 1 mmol/L sodium orthovanadate, pH 10, 1 mmol/L EDTA, 1 mmol/L EGTA, 10 mmol/L sodium β-glycerophosphate, 50 mmol/L NaF, 5 mmol/L sodium pyrophosphate, 1% [w/v] Triton X-100, 0.1% [v/v] 2-mercaptoethanol, one tablet of complete TM protease inhibitor [Roche, Burgess Hill, U.K.]) and subjected to Western blotting. Primary antibodies were anti-PKAβcat (1:1,000) (Santa Cruz Biotechnology, Santa Cruz, CA), anti–phospho-ERK thr^{202} tyr^{204} (1:1,000), anti-ERK1/2 native (1:1,000), and anti–β-actin (1:1,000) (Cell Signaling Technologies, Beverley, U.K.). HRP–anti-rabbit IgG (1:1,000) was used as a secondary antibody with enhanced chemiluminescence (Amersham, Little Chalfont, U.K.) and exposure to Amersham HyperfilmTH ECL autoradiographic film (Amersham). Blots were quantified using ImageJ software (www.ncbi.nlm.nih.gov).

Optical projection tomography. Optical projection tomography (OPT) was performed on whole pancreata (14) using an OPT scanner (Bioptonics 3001; Skyscan, Kontich, Belgium) and images were analyzed with Data Viewer version 1.3.2 (Bioptonics).

Immunostaining. Whole pancreata were fixed (4% paraformaldehyde), wax embedded, and sectioned (5 μm) before being immunostained with sheep anti-HSD1 antibody (13). For chromogen labeling with diaminobenzidine (DakoCytomation, Inc, Carpinteria, CA), biotinylated anti-sheep (Abcam, plc, Cambridge, U.K.) was used as secondary antibodies. Images were processed using KS3000 software (version 3.0; Carl Zeiss Vision, GmbH).

Immunofluorescence staining. Frozen sections (5 μm) of whole pancreata or single cells from trypsin-digested islets were fixed in acetone:methanol (90:10 v/v) and immunostained using guinea pig anti-insulin, sheep anti–11β-HSD1 antibody (13), rabbit anti-glucagon, somatostatin, pancreatic polypeptide (Chemicon; Millipore, Billerica, MA), and Cy2-conjugated AffiniPure F(ab')$_2$ fragment donkey anti–guinea pig IgG, rhodamine red X–conjugated AffiniPure F(ab')$_2$ fragment donkey anti-sheep, fluorescein isothiocyanate–conjugated AffiniPure F(ab')$_2$ fragment donkey anti-sheep, and rhodamine red X–conjugated AffiniPure F(ab')$_2$ fragment donkey anti-rabbit (Jackson ImmunoResearch Laboratories, Inc., West Grove, PA) were used as secondary antibodies. Images were taken using a Leica confocal microscope linked to LSM Image Browser software.

Insulin content. Whole pancreata were homogenized in lysis buffer, and insulin was extracted with acid ethanol and measured by radioimmunoassay (Linco Research). Insulin was normalized to total protein content (Bio-Rad Laboratories, Hercules, CA).

Statistics. Data are expressed as mean ± SEM and were analyzed by unpaired Student *t* test, one-way ANOVA Newman-Keuls, or two-way ANOVA.

RESULTS

Generation of β-cell–specific 11β-HSD1 overexpression model. The rat 11β-HSD1 cDNA was cloned downstream of the mouse insulin I promoter (Fig. 1*A*) that drives highly β-cell–specific expression (10,15). The construct was validated by demonstrating increased 11β-HSD1 activity after transfection into clonal INS1E and MIN6 cells (Supplementary Fig. 1*A* and *B*). Transgenic mice were generated on the β-cell, failure-susceptible C57BL/KsJ (KsJ) strain background (11). Southern blotting suggested integration of a low copy number (approximately two) of the transgene (Fig. 1*B*). In MIP-HSD1$^{tg/+}$ islets, 11β-HSD1 mRNA was increased eightfold (Fig. 1*C*). 11β-HSD1 protein was elevated specifically in β-cells of MIP-HSD1 transgenics (Fig. 1*D* and Supplementary Fig. 2). Note that 11β-HSD1 is expressed in β-cells of normal islets, as shown by the colocalization with insulin-positive cells and in other islet cell subtypes (Supplementary Fig. 3), as found by others (16). 11β-HSD1 reductase (glucocorticoid reactivation) activity was approximately twofold higher in isolated primary MIP-HSD1$^{tg/+}$ islets than littermate control islets and was glucose inducible (Fig. 1*E*). Hexose-6-phosphate dehydrogenase level, which drives 11β-reductase activity (17), was not limiting. 11β-HSD1 dehydrogenase (glucocorticoid inactivating) activity was 10-fold lower than reductase in islets and was unaffected by transgene or high glucose (Supplementary Fig. 1*C* and *D*). MIP-HSD1$^{tg/+}$ mice were viable and appeared grossly normal (Table 1). Fasting plasma insulin, glucose triglyceride, and NEFA levels were unaffected by genotype (Table 1), indicating similar peripheral insulin sensitivity and β-cell exposure to lipotoxicity with HF.

MIP-HSD1$^{tg/+}$ mice are protected from HF diet–induced β-cell failure. To determine transgene impact in vivo, mice were fed an HF diet for 12 weeks to induce β-cell failure (11). Plasma corticosterone levels were not significantly affected by diet or genotype (Table 1), indicating that transgene effects were β-cell specific and not due to

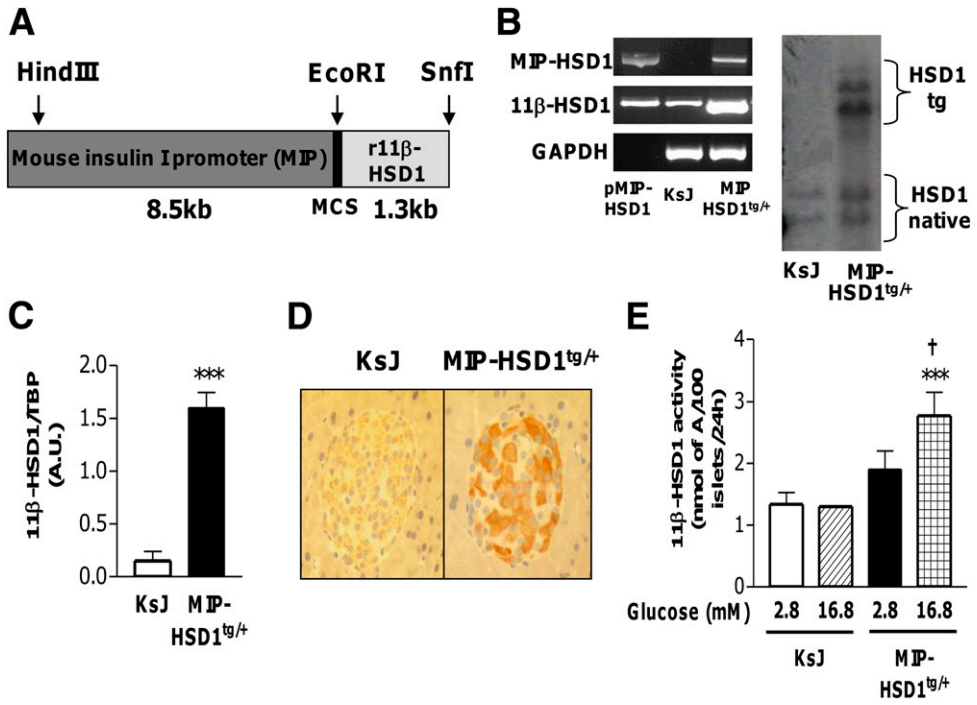

FIG. 1. Validation of the MIP-HSD1 transgenic model. *A*: Schematic representation of the MIP-HSD1 transgene. *B*: Germline transmission was confirmed using PCR of tail DNA using MIP-HSD1–specific primers and glyceraldehyde-3-phosphate dehydrogenase (GAPDH) as an internal control. The left panel shows PCR bands in pMIP-HSD1 plasmid control and MIP-HSD1 DNA, but not KsJ genomic DNA. The right panel shows Southern analysis with clear signal from endogenous 11β-HSD1 (lower bands) and the MIP-HSD1 transgene (upper bands). Copy number was two to four in MIP-HSD1$^{tg/+}$. *C*: 11β-HSD1 mRNA levels measured by real-time PCR in isolated islets of either KsJ or MIP-HSD1$^{tg/+}$; $n = 8$. ***$P < 0.001$. *D*: Representative immunohistochemistry images showing 11β-HSD1 localization in islets from KsJ and MIP-HSD1$^{tg/+}$ mice. Original magnification ×40. *E*: 11β-HSD1 activity assayed in isolated islets from KsJ and MIP-HSD1$^{tg/+}$ mice treated with low (2.8 mmol/L) or high (16.8 mmol/L) glucose concentrations expressed as nanomoles of 11-DHC [A] metabolized into corticosterone [B] after 24 h. ***$P < 0.001$, MIP-HSD1$^{tg/+}$ 16.8 mmol/L vs. KsJ 16.8 mmol/L; $n = 6$. †$P < 0.05$, MIP-HSD1$^{tg/+}$ 16.8 mmol/L vs. MIP-HSD1$^{tg/+}$ 2.8 mmol/L; $n = 6$. a.u., arbitrary units. (A high-quality digital representation of this figure is available in the online issue.)

hypothalamic-pituitary-adrenal disturbance. To accurately assess insulin secretion, especially over the rapid response of the first phase (1–10 min), glucose was infused through a jugular cannula. CD-fed animals had comparable responses to glucose infusion (Fig. 2*A* and *C*). HF-fed KsJ mice, as expected (11), showed markedly attenuated GSIS indicative of β-cell failure and an associated prolonged elevation of plasma glucose levels in vivo (Fig. 2*B* and *C*). In contrast, HF-fed MIP-HSD1$^{tg/+}$ mice exhibited profoundly elevated first- and second-phase GSIS that completely normalized glucose levels (Fig. 2*B* and *C*).

MIP-HSD1$^{tg/+}$ mice have increased adult islet number. Protective MIP-HSD1$^{tg/+}$ compensatory hyperinsulinemia can occur through two major pathways: increased β-cell number (neogenesis, β-cell replication, and reduced apoptosis) and increased β-cell function (insulin output per β-cell). To address β-cell/islet number, whole pancreas islet number was quantified by OPT (14) (Fig. 3*A* and *B*) and validated by conventional immunohistochemistry in pancreas sections (Fig. 3*C*). MIP-HSD1$^{tg/+}$ had more islets (Fig. 3*A*–*C*) of smaller dimensions compared with littermates on control and HF diet (Fig. 3*D*). Average islet size increased

TABLE 1
Physiological parameters of MIP-HSD1 mice

	KsJ CD	KsJ HF	MIP$^{tg/+}$ CD	MIP$^{tg/+}$ HF	MIP$^{tg/tg}$ CD	MIP$^{tg/tg}$ HF
Body weight (g)	29.1 ± 0.36	30.0 ± 0.38	30.0 ± 0.39	29.5 ± 0.42	30.2 ± 0.4	29.2 ± 0.3
Food intake (kcal/mice/day)	12.8 ± 3.1	11.1 ± 1.5	13.2 ± 2.0	11.9 ± 0.8	10.2 ± 1.3	11.8 ± 1.0
Epididymal mass (mg/g body weight)	19.5 ± 1.9	28.3 ± 1.8**	17.1 ± 1.4	23.8 ± 1.7*	14.2 ± 1.4	22.6 ± 1.3*
Liver mass (mg/g body weight)	46.6 ± 1.4	44.2 ± 1.3	40.8 ± 2.1	45.1 ± 1.6	39.4 ± 2.16	41 ± 2.3
Fasting glucose (mmol/L)	5.4 ± 0.32	5.6 ± 0.48	4.89 ± 0.6	5.2 ± 0.24	5.3 ± 0.3	5.25 ± 0.3
Fasting insulin (ng/mL)	0.85 ± 0.33	0.48 ± 0.27	0.56 ± 0.11	0.74 ± 0.33	0.56 ± 0.35	0.43 ± 0.17
Fasting NEFA (mmol/L)	0.94 ± 0.04	1.27 ± 0.18	1.10 ± 0.10	1.48 ± 0.20	1.08 ± 0.12	1.18 ± 0.05
Fed NEFA (mmol/L)	0.33 ± 0.06	0.68 ± 0.06**	0.34 ± 0.06	0.58 ± 0.07*	0.27 ± 0.04	0.67 ± 0.14*
Fasting triglyceride (mmol/L)	0.97 ± 0.03	0.94 ± 0.03	0.88 ± 0.02	0.89 ± 0.02	0.96 ± 0.01	0.93 ± 0.01
Fed triglyceride (mmol/L)	0.97 ± 0.05	1 ± 0.05	0.92 ± 0.02	0.91 ± 0.02	0.86 ± 0.02	0.94 ± 0.02
Corticosterone level (ng/mL)	6.87 ± 1.5	9.46 ± 2.2	4.98 ± 0.9	9.60 ± 1.4	4.49 ± 0.6	5.11 ± 0.7

Data are mean ± SEM. Body weight, food intake, tissue weights, fasting glucose, insulin, fasting and fed triglycerides, NEFA, and morning corticosterone levels in 3-month-old male KsJ, MIP-HSD1$^{tg/+}$, and MIP-HSD1$^{tg/tg}$ mice after 12 weeks on CD or HF diet. *$P < 0.05$ vs. CD; n = 9–12. **$P < 0.01$ vs. CD; n = 9–12.

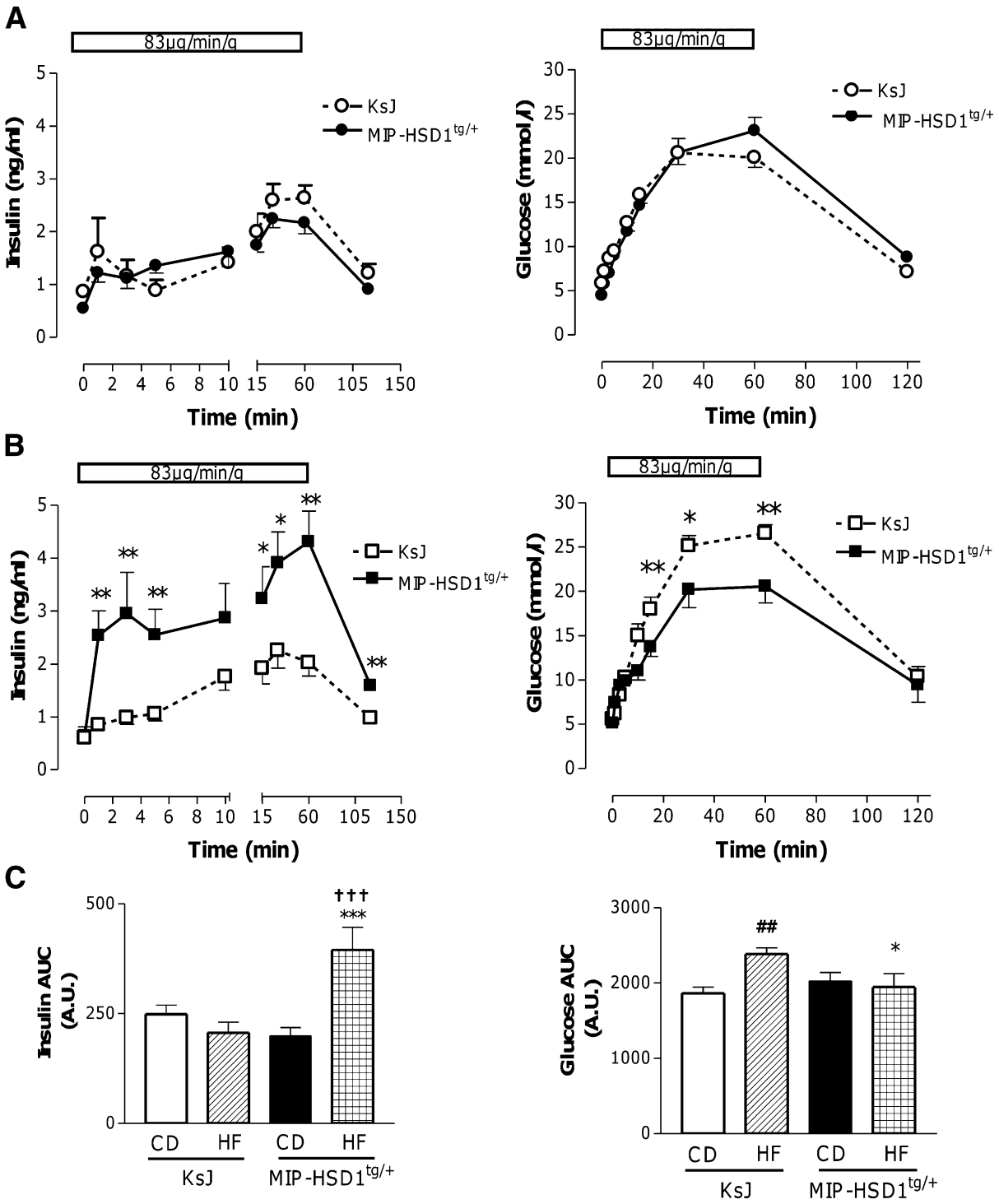

FIG. 2. Reversal of β-cell failure in MIP-HSD1$^{tg/+}$ mice in vivo. *A*: CD-fed KsJ and MIP-HSD1$^{tg/+}$ mice were infused with glucose (83 µg/min/g) for 1 h intravenously to test dynamic first- and second-phase β-cell insulin secretion (*left*) and associated glycemia (*right*) in vivo. *B*: Data for HF-fed KsJ and MIP-HSD1$^{tg/+}$ mice as in *A*. *$P < 0.05$; **$P < 0.01$, between MIP-HSD1$^{tg/+}$ HF vs. HF KsJ. *C*: Area under the curve for insulin (*left*) and glucose (*right*). ***$P < 0.001$, MIP-HSD1$^{tg/+}$ HF vs. KsJ HF. †††$P < 0.001$, MIP-HSD1$^{tg/+}$ HF vs. MIP-HSD1$^{tg/+}$ CD. ##$P < 0.01$, KsJ HF vs. KsJ CD. *$P < 0.05$, between MIP-HSD1$^{tg/+}$ HF vs. KsJ HF. n = 6–9. A.U., arbitrary units.

in KsJ mice with chronic HF, indicating selective loss of small functional islets (Fig. 3*A–D*), a process driven at least in part by apoptosis (18), whereas MIP-HSD1$^{tg/+}$ mice showed attenuation of β-cell loss. β-Cell replication (as indicated by Pdx1 and Ki67 costaining) was unaltered in MIP-HSD1$^{tg/+}$ transgenics (Supplementary Fig. 4). The insulin promoter is expressed at an early stage of pancreatic islet development (19) when increased glucocorticoid exposure reduces β-cell mass (20). This would predict, if anything, lower islet mass in MIP-HSD1$^{tg/+}$ mice. However, the MIP-HSD1 transgene had no discernible effect on the development of the endocrine pancreas (OPT in fetal day E18 islet bodies and newborn pancreas) (Supplementary Fig. 5), suggesting that a postnatal regulatory

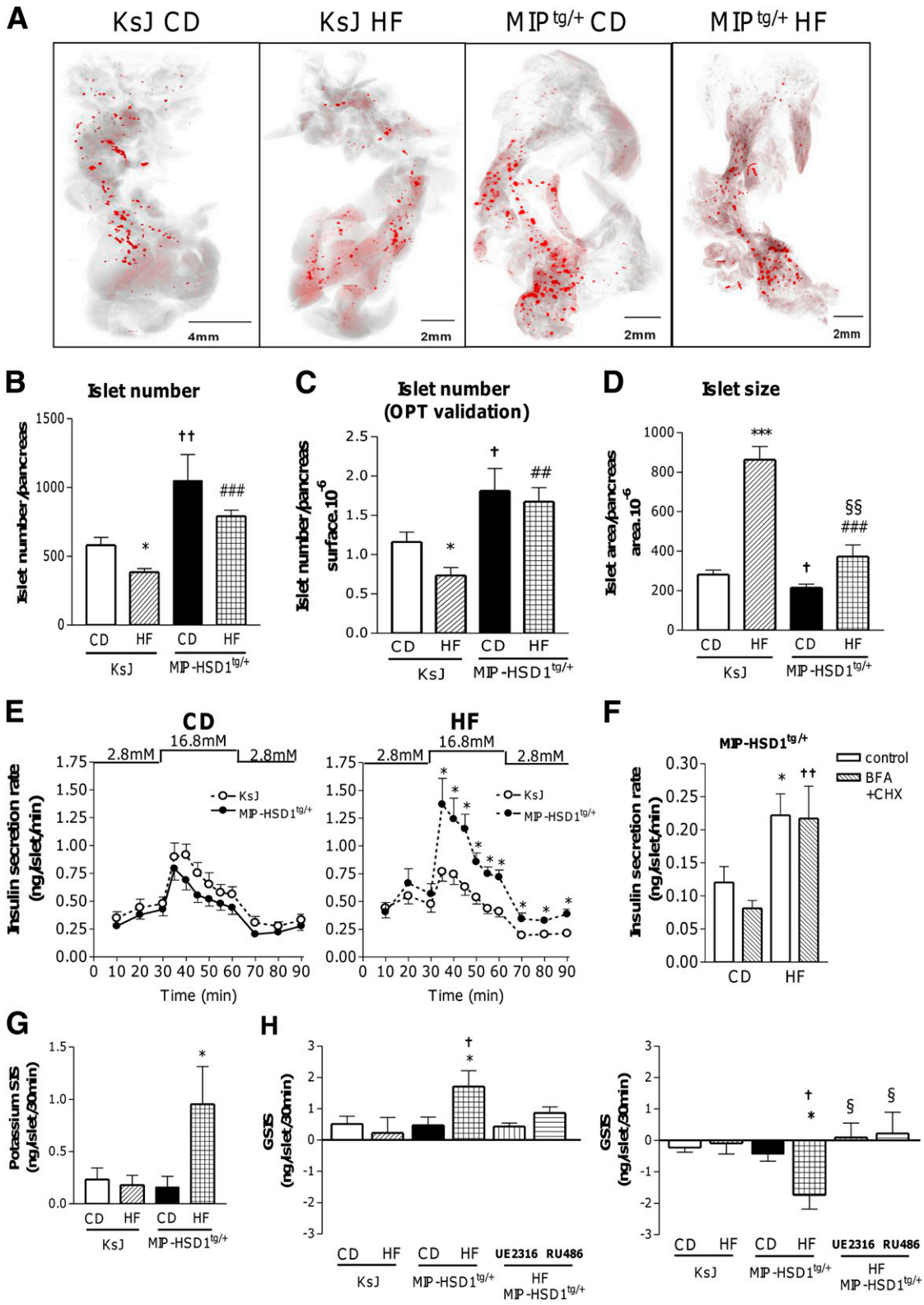

FIG. 3. Augmented islet number and function in HF-fed MIP-HSD1$^{tg/+}$ mice. *A*: Representative OPT images of whole pancreas from KsJ and MIP-HSD1$^{tg/+}$ mice after 12 weeks on CD or HF diet. Insulin fluorescent immunostaining is represented by red coloring. *B*: Quantification by OPT of insulin-positive islets per whole pancreas in KsJ and MIP-HSD1$^{tg/+}$ mice on CD or HF diet. *$P < 0.05$, KsJ CD vs. KsJ HF. ††$P < 0.01$, MIP-HSD1$^{tg/+}$ CD vs. KsJ CD. ###$P < 0.001$, MIP-HSD1$^{tg/+}$ HF vs. KsJ HF. n = 4–6. *C*: The OPT method was validated by determining the ratio of islet number per pancreatic surface area in pancreatic sections immunostained for insulin. *$P < 0.05$, KsJ CD vs. KsJ HF. ##$P < 0.01$, MIP-HSD1$^{tg/+}$ HF vs. KsJ HF. †$P < 0.05$, MIP-HSD1$^{tg/+}$ vs. KsJ CD. n = 15–20 sections per pancreas; n = 12–15 mice per group. *D*: Islet size (ratio of islet area to total pancreatic surface area; μm^2) in pancreatic sections immunostained for insulin. ***$P < 0.001$, KsJ CD vs. KsJ HF. †$P < 0.05$, MIP-HSD1$^{tg/+}$ CD vs. KsJ CD. ###$P < 0.001$, MIP-HSD1$^{tg/+}$ HF vs. KsJ HF. §§$P < 0.01$, MIP-HSD1$^{tg/+}$ HF vs. MIP-HSD1$^{tg/+}$ CD. n = 20–15 sections per pancreas; n = 15–20 mice per group. *E*: GSIS from batches of 10 size-matched islets from CD-fed (*left*) or HF-fed (*right*) KsJ and MIP-HSD1$^{tg/+}$ mice exposed to 2.8 mmol/L and then 16.8 mmol/L glucose. *$P < 0.05$, MIP-HSD1$^{tg/+}$ HF vs. KsJ HF (n = 6). *F*: Basal insulin secretion by islets from KsJ and MIP-HSD1$^{tg/+}$ mice on CD or HF diet were preincubated for 2 h in 2.8 mmol/L glucose with or without 0.5 μg/mL BFA and 15 μmol/L CHX and then incubated for 30 min with

mechanism drives increased islet number in MIP-HSD$^{tg/+}$ mice.

MIP-HSD1$^{tg/+}$ mice have augmented islet-autonomous secretory function. To test the additional possibility of enhanced islet insulin secretory function, we measured GSIS in carefully size-matched (average diameter 100 μm) isolated islets in vitro. In agreement with the findings in vivo, isolated islets from CD-fed KsJ and MIP-HSD1$^{tg/+}$ mice showed similar GSIS (Fig. 3*E*, left), whereas islets from HF-fed MIP-HSD1$^{tg/+}$ mice exhibited augmented GSIS (Fig. 3*E*, right).

MIP-HSD1$^{tg/+}$ islets have augmented membrane-proximal secretory capacity. We next investigated whether the insulin secretory machinery was specifically enhanced in MIP-HSD1$^{tg/+}$ islets. To assess this, insulin translation and Golgi trafficking was inhibited with CHX and brefeldin A (BFA), revealing relatively enhanced basal (unregulated) insulin secretion from islets of MIP-HSD1$^{tg/+}$ mice on HF compared with control-fed mice (Fig. 3*F*). In addition, PSIS (glucose independent, membrane proximal) was significantly higher from islets of HF-fed MIP-HSD1$^{tg/+}$ compared with HF-fed KsJ mice (Fig. 3*G*), consistent with a larger pool of secretory granules and/or a faster rate of exocytosis in islets of MIP-HSD1$^{tg/+}$ mice on HF.

11β-HSD1/glucocorticoid–dependent effects on islet function are dose sensitive. To confirm glucocorticoid and 11β-HSD1 dependence of the transgene, islets were incubated acutely (2 h) in 20 nmol/L (~physiological) or 200 nmol/L (supraphysiological) 11-DHC. GSIS was significantly higher from islets from HF MIP-HSD1$^{tg/+}$ mice exposed to 20 nmol/L 11-DHC, and this was abolished by the 11β-HSD1 inhibitor UE2316 (Supplementary Table 1) and the GR antagonist RU486. Supraphysiological 11-DHC completely blunted GSIS, as mentioned by others (4,6,16). Inhibition was also reversed in islets of HF-fed MIP-HSD1$^{tg/+}$ mice by 11β-HSD1 and GR inhibitors.

Palmitate-stimulated GSIS is augmented in MIPHSD1$^{tg/+}$ islets in vitro. Fatty acids augment insulin secretion in the short term. To investigate the role of elevated β-cell 11β-HSD1 in this process, palmitate-stimulated GSIS was assessed in isolated islets from MIP-HSD1$^{tg/+}$ after 24 h exposure to 20 nmol/L 11-DHC. Notably, long-term static exposure of islets to 20 nmol/L 11-DHC alone impaired insulin release in vitro (Supplementary Fig. 8). Palmitate-stimulated GSIS from MIP-HSD$^{tg/+}$ was reversed by 11β-HSD1 and GR inhibitors (Supplementary Fig. 8), suggesting a role for 11β-HSD1 in fatty acid–stimulated GSIS.

MIP-HSD1$^{tg/+}$ islets show induction of genes of differentiation, secretory pathways, and cellular stress management. To better understand the mechanisms of improved islet function in HF-fed MIP-HSD1$^{tg/+}$ mice, we performed a comparative transcriptomic analysis (Supplementary Table 2). MIP-HSD1$^{tg/+}$ islets had higher mRNA levels for genes of the small GTPase pathway (*Arf6*, *Prkacb*, and PKA catalytic subunit β [*PKAβcat*]) linked to enhanced insulin secretion and islet survival (21–23), protein trafficking, turnover, and vesicle docking (*VapB* and *C*, *Arf6*, *cplx2*, and *stx11*), consistent with the enhanced secretory responses (Fig. 3*E*, right, and *F* and *G*) and the mitogen-activated protein kinase/extracellular signal–related kinase (ERK) (*B-raf*, *Max*, and *Cdkn1a/p21*) and Jak/Stat pathways (*Ccnd2* and *Jak1*), indicative of maintained differentiation versus proliferation commitment (24–27) and protection from apoptosis (28,29). MIP-HSD1$^{tg/+}$ islets also exhibited higher mRNA levels of genes related to protection from cellular stress (*hspa1a*, *-a1b*, *-a4*, and *trib3*) (30). Key gene expression changes were validated by real-time PCR (Fig. 4*A–D*). Interestingly, *Cdkn1a* gene expression was downregulated in islets of KsJ mice on HF (Fig. 4*D*), consistent with HF-induced cellular stress, apoptosis (29), and islet loss (Fig. 3*A–C*), whereas *Cdkn1a* was upregulated by HF in MIP-HSD1$^{tg/+}$, consistent with maintained functionality with reduced cellular stress.

MIP-HSD1$^{tg/+}$ islets exhibit elevated PKA and ERK signaling. To test whether the validated gene expression changes had a functional impact upon islet responses, we investigated two key pathways linked to enhanced insulin secretion (PKA) and downstream cell differentiation/survival pathways (ERK). Protein levels of the catalytic subunit of PKA (PKAβcat) were markedly induced in islets from HF diet–fed MIP-HSD1$^{tg/+}$ mice (Fig. 4*E*), and this was reversed with the 11β-HSD1 inhibitor UE2316 (Fig. 4*F*) but not the PKA phosphorylation inhibitor KT5720 (Fig. 4*G*). Likewise, activation (phosphorylation) of the ERK signaling pathway was enhanced in MIP-HSD1$^{tg/+}$ islets (Fig. 4*H*). Induction of ERK activation in MIP-HSD1$^{tg/+}$ islets was abolished by UE2316 (Fig. 4*I*), confirming enzyme specificity. The increased ERK phosphorylation in MIP-HSD1$^{tg/+}$ islets was also abolished in the presence of the PKA inhibitor KT5720 (Fig. 4*J*), as expected.

11β-HSD1$^{-/-}$ mice have mildly impaired β-cell function offset by improved glucose tolerance. We next investigated whether 11β-HSD1 deficiency impacted GSIS with HF feeding. 11β-HSD1$^{-/-}$ mice exhibited a blunted early-phase GSIS and mild transient glucose intolerance in vivo (Supplementary Fig. 6*A* and *B*). Note that glucose/insulin homeostasis in 11β-HSD1$^{-/-}$ mice is comparable to control C57BL/6J mice when on CD (12), indicating a β-cell–specific defect. However, insulin secretion was markedly lower in HF-fed 11β-HSD1$^{-/-}$ than C57BL/6J mice in association with markedly improved glucose tolerance (Supplementary Fig. 6*C* and *D*), suggesting substantially reduced secretory demand from β-cells due to the dominant protection from glucose intolerance in HF-fed 11β-HSD1$^{-/-}$ mice.

Partially impaired insulin secretion in MIP-HSD1$^{tg/tg}$ mice indicates a threshold effect for 11β-HSD1–mediated β-cell compensation. Glucocorticoids sometimes show complex dose-related effects (31) (Fig. 3*H*). To address this, we analyzed insulin secretion in homozygous MIP-HSD1$^{tg/tg}$ mice with ~16-fold higher islet 11β-HSD1 mRNA and ~4-fold higher 11β-HSD1 activity (Supplementary Fig. 7*A* and *B*). In contrast to MIP-HSD1$^{tg/+}$, MIP-HSD1$^{tg/tg}$ mice exhibited a significant reduction of whole pancreas insulin content and marked suppression of GSIS on normal diet in vivo, although normal glucose tolerance was

BFA/CHX in 2.8 mmol/L glucose in order to stop both neosynthesis of insulin and neoformation of newly formed insulin vesicles. *$P < 0.05$, MIP-HSD1$^{tg/+}$ HF vs. MIP-HSD1$^{tg/+}$ CD. ††$P < 0.01$, treated MIP-HSD1$^{tg/+}$ HF vs. treated MIP-HSD1$^{tg/+}$ CD. $n = 4$. *G*: PSIS from islets of KsJ and MIP-HSD1$^{tg/+}$ mice on CD or HF diet incubated for 30 min in 2.8 mmol/L glucose and then 30 min with 40 mmol/L KCl. *$P < 0.05$, MIP-HSD1$^{tg/+}$ HF vs. KsJ HF. $n = 6$. *H*: GSIS from islets of KsJ and MIP-HSD1$^{tg/+}$ mice on CD or HF diet preincubated for 2 h with 20 nmol/L 11-DHC (*left*) or 200 nmol/L 11-DHC (*right*) with or without 1 μmol/L UE2316 or 1 μmol/L RU486 before incubation for 30 min with 2.8 mmol/L glucose followed by 30 min with 16.8 mmol/L glucose. *$P < 0.05$, MIP-HSD1$^{tg/+}$ HF vs. Ksj HF. †$P < 0.05$, MIP-HSD1$^{tg/+}$ HF vs. MIP-HSD1$^{tg/+}$ CD. §$P < 0.05$, MIP-HSD1$^{tg/+}$ HF treated vs. MIP-HSD1$^{tg/+}$ HF. $n = 5–6$. (A high-quality digital representation of this figure is available in the online issue.)

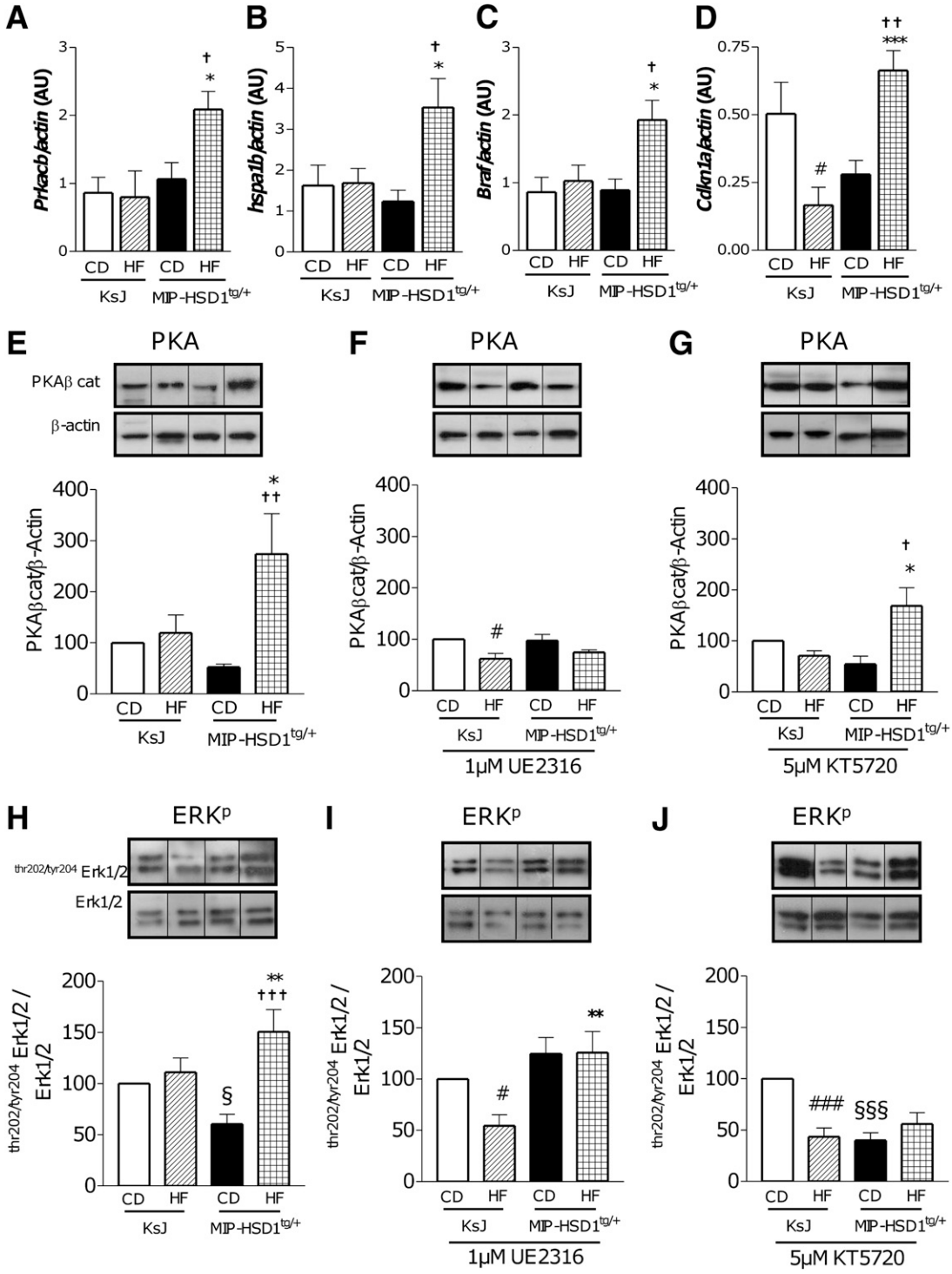

FIG. 4. Validation of selected genes changes from microarray functional clusters at the mRNA, protein, and protein phosphorylation level associated with improved islet function in HF-fed MIP-HSD1$^{tg/+}$. *Prkacb* (*A*), *hspa1b* (*B*), *Braf* (*C*), and *Cdkn1a* (*D*) mRNA expression was measured in isolated islets of KsJ and MIP-HSD1$^{tg/+}$ mice on CD or HF diet and normalized to gene expression of actin. *$P < 0.05$; ***$P < 0.001$, MIP-HSD1$^{tg/+}$ HF vs. KsJ HF. #$P < 0.05$, KsJ HF vs. KsJ CD. †$P < 0.05$, ††$P < 0.01$, MIP-HSD1$^{tg/+}$ HF vs. MIP-HSD1$^{tg/+}$ CD. $n = 6$–8 (2–3 mice per islet preparation). AU, arbitrary units. Isolated islets from KsJ and MIP-HSD1$^{tg/+}$ mice on CD or HF diet were incubated in the absence (*E* and *H*) or presence of 1 μmol/L of the selective 11β-HSD1 inhibitor UE2316 (*F* and *I*) or 5 μmol/L PKA inhibitor KT5720 (*G* and *J*) for 24 h. Total extracts were subjected to immunoblotting analysis for PKAβ catalytic subunit and β-actin (loading control) (*E–G*), thr^{202}/tyr^{204}ERK1/2 phosphorylation, and ERK1/2 native protein (*H–J*). Representative images of the blots are shown above the quantification. Quantitative analysis shows protein expression level normalized to the respective control proteins and then expressed relative to the values in the KsJ control mice. Note that proteins from CD mice were run on separate gels from HF mice together with the same internal control, which allowed signal comparison. *$P < 0.05$; **$P < 0.01$, MIP-HSD1$^{tg/+}$ HF vs. KsJ HF. †$P < 0.05$; ††$P < 0.01$; †††$P < 0.001$, MIP-HSD1$^{tg/+}$ HF vs. MIP-HSD1$^{tg/+}$ CD. #$P < 0.05$; ###$P < 0.001$, KsJ HF vs. KsJ CD. §$P < 0.05$; §§§$P < 0.001$, MIP-HSD1$^{tg/+}$ CD vs. KsJ CD. $n = 6$.

maintained (Supplementary Fig. 7*C*, *D*, and *F*). However, MIP-HSD1$^{tg/tg}$ mouse GSIS was comparable to littermates on HF diet (Supplementary Fig. 7*E*, left, and *F*, left), reflecting a relative improvement in GSIS versus CD, and this partially normalized glucose tolerance (Supplementary Fig. 7*E*, right, and *F*, right). In agreement with this intermediate phenotype, GSIS from isolated islets of HF-fed MIP-HSD1$^{tg/tg}$ mice showed a higher basal and peak secretion, although this was not sustained over the whole second phase (Supplementary Fig. 7*F*).

Islet 11β-HSD1 level is predictive of β-cell compensatory capacity and diabetes susceptibility in mice. Considering the inverted U-shaped MIP-HSD1 gene dose-response effect on β-cell secretory function, we assessed islet 11β-HSD1 protein and activity levels in contrasting models of β-cell failure (HF-fed KsJ and Lep$^{db/db}$ mice) and β-cell compensation (C57BL/6J mice). HF induced a modest elevation of 11β-HSD1 in islets from robustly compensating C57BL/6J mice (Fig. 5*A* and *B*). In contrast, down-regulation of islet 11β-HSD1 was found in β-cell failure–susceptible, HF-fed KsJ mice (Fig. 5*C* and *D*). Markedly high 11β-HSD1 levels were found in diabetic Lep$^{db/db}$ islets (Fig. 5*E* and *F*).

DISCUSSION

Our data show that, for the first time, an unexpectedly beneficial metabolic outcome results from optimal elevation of β-cell 11β-HSD1, in contrast to the diabetogenic effects of elevated 11β-HSD1 in adipose tissue and liver (3). Moreover, this effect may be physiologically relevant, as normal mice that exhibit robust compensatory insulin secretion on HF exhibit a similar modest upregulation of β-cell 11β-HSD1. A higher or lower 11β-HSD1 level suppresses GSIS, consistent with an inverted U-shaped dose-response effect sometimes seen with glucocorticoids (31). This notion is supported by the stimulatory effect of physiological 11β-HSD1 substrate (11-DHC) but suppressive effects of high or indeed long-term exposure to 11-DHC in vitro. In agreement, diabetic Lep$^{db/db}$ mice (32) and MIP-HSD1$^{tg/tg}$ on CD have impaired GSIS in vivo associated with more marked elevation of β-cell 11β-HSD1. These data are also consistent with the association between increasing 11β-HSD1 levels and the severity of hyperglycemia in diabetic *fa/fa* rats (5). Conversely, 11β-HSD1$^{-/-}$ mice on CD and KsJ mice on HF diet have β-cell secretory defects associated with the absence or decrease of 11β-HSD1 activity, respectively. These findings may have implications

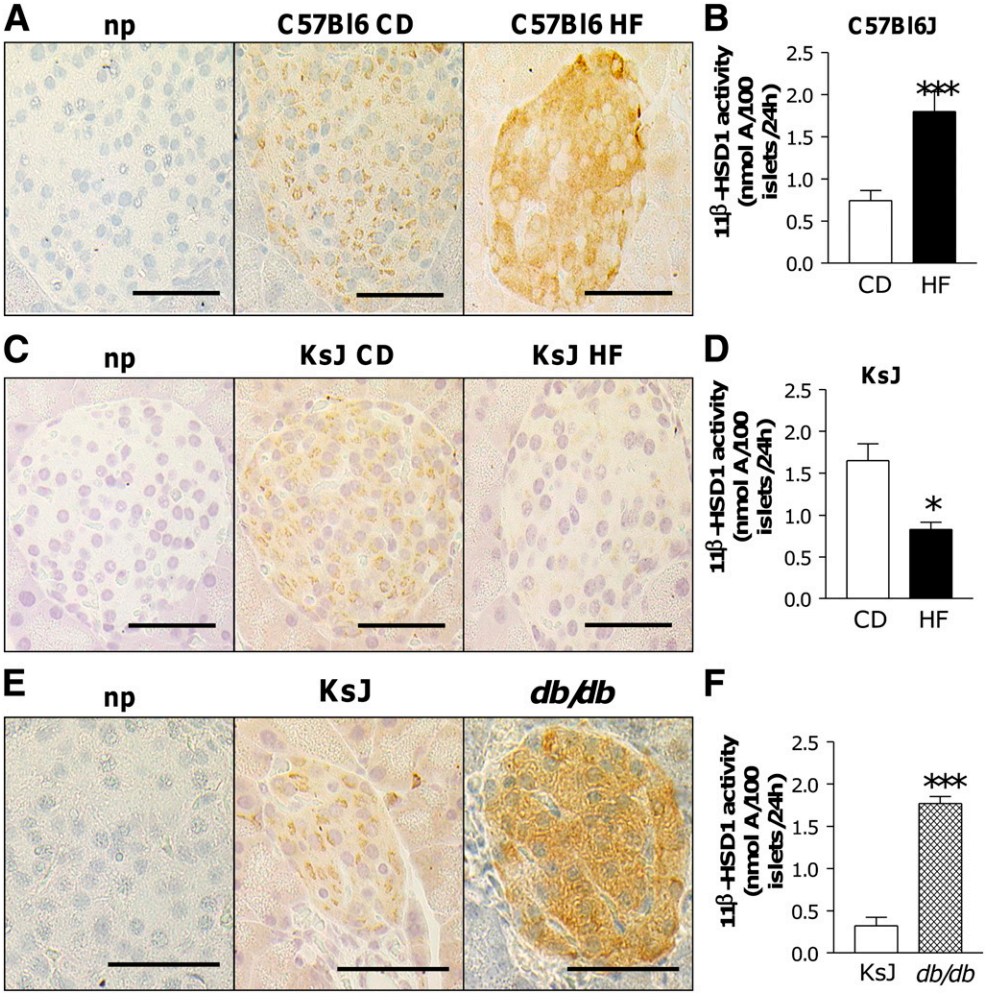

FIG. 5. Islet 11β-HSD1 protein and activity levels relate to β-cell compensation in different mouse strains. Representative images showing 11β-HSD1 localization throughout the islet (largely β-cells) by immunohistochemistry in pancreas from C57BL/6J mice that exhibit compensatory insulin secretion (*A*), β-cell failure–prone KsJ on either CD or HF diet (*C*), and control KsJ wild-type or diabetic KsJ-*Lep*$^{db/db}$ mice (*E*). Original magnification ×40. np, no primary antibody control. Proportionately altered 11β-HSD1 activity was confirmed in isolated islets from the respective models: C57BL/6J (*B*) and KsJ (*D*) on either CD or HF diet. **P* < 0.05; *n* = 3. ****P* < 0.001; *n* = 9. *F*: KsJ wild-type and diabetic KsJ-*Lep*$^{db/db}$ mice. ****P* < 0.001; *n* = 6. (A high-quality digital representation of this figure is available in the online issue.)

for the timing and dose of steroid or 11β-HSD1 inhibitor interventions in the therapeutic treatment of patients predisposed to β-cell failure. Defining the impact of altered islet 11β-HSD1 expression across the progression from glucose intolerance, prediabetes, and frank diabetes in both rodent models and humans, relative to peripheral tissue 11β-HSD1 levels, will be of future importance to assess any adverse risks of therapeutic inhibition. However, the dominant protection from glucose intolerance found in HF-fed 11β-HSD1$^{-/-}$ mice indicates that beneficial effects of 11β-HSD1 inhibition may outweigh any detrimental effect on β-cells.

The gene-dose, inverted-U effect of the MIP-HSD1 transgene may reconcile conflicting reports of suppressive (4–8) versus stimulatory effects (33–35) of glucocorticoids on insulin secretion. Thus, the prevailing effect is likely a function of dose and duration. Indeed, although our in vitro data are generally supportive of our in vivo findings, we note that long-term, but not short-term, static incubation with low 11-DHC is suppressive. We contend that static incubation with steroids and isolated islets in vitro does not reflect dynamic glucocorticoid exposure/metabolism patterns found in vivo. This merely serves to underline the importance of studying the impact of altered β-cell 11β-HSD1 in the whole animal chronic disease context. Of note, β-cell–specific GR overexpression (RIP-GR) causes direct suppression of insulin secretion (7). Beyond exposure and dose issues, this suggests that MIP-HSD1 effects could result from additional effects beyond GR activation. For example, physiological corticosterone binds with high affinity to mineralocorticoid receptors, which antagonizes GR-mediated suppression of insulin secretion and may thus contribute to beneficial (36) and dose-sensitive effects. Notably, the synthetic GR-selective glucocorticoid dexamethasone, commonly used in in vitro islet studies, is a poor 11β-HSD1 substrate, perhaps further explaining differences between solely GR- versus 11β-HSD1–mediated effects in islets. 11β-HSD1 reductase activity depletes endoplasmic reticulum (ER) NADPH, but this does not appear to affect the increased cytosolic NADPH levels required to activate GSIS (37). Elevated 11β-HSD1 may also preferentially amplify nongenomic effects of glucocorticoids (38) more than GR overexpression, or indeed non-GR effects due to alternative substrate metabolism (39) by 11β-HSD1. Indeed, alternate 11β-HSD1 metabolites (40) may affect GSIS through oxysterol activation of nuclear liver X receptor (41). Finally, RIP-GR mice may manifest impaired GSIS as a result of developmentally impaired β-cell mass (20), unlike the MIP-HSD1 model. In any case, there is more evidence to suggest that islet 11β-HSD1, rather than GR, levels are elevated in islets from diabetic mice (5,6, and the current study), suggesting the MIP-HSD1 mice are perhaps a more relevant in vivo model. Crucially, the unexpected augmentation of GSIS in the MIP-HSD1 mice due to chronic modest elevation of β-cell 11β-HSD1 in vivo has allowed us to challenge prevailing hypotheses on glucocorticoid-mediated diabetogenic effects in islets. Those hypotheses are derived from arguably artificial systems such as systemic administration of high-dose steroids in vivo, which induces confounding peripheral insulin resistance, as well as the effects of acute and often pharmacological steroid concentrations in islets in vitro.

Elevated expression of genes involved in differentiation, insulin secretion, and cellular stress protection and survival are associated with augmented MIP-HSD1$^{tg/+}$ islet function. Although similar effects of glucocorticoids have been noted in other cellular systems, our data show these effects for the first time, to our knowledge, in pancreatic islets, and highlight novel areas of cross-talk in this cell type. Thus, glucocorticoids curtail proliferation and induce differentiation, in part through the increased cyclin-dependent kinase inhibitor 1A (p21) (24,26,27,42) and enhanced differentiation through ERK1/2 (26). Increased v-raf murine sarcoma viral oncogene homolog B1 (B-Raf) signaling (43) and enhanced PKAβcat and small GTPase activation makes a clear mechanistic link with augmented insulin secretory capacity (21,25,43) as well as islet survival in the face of HF diet–induced ER stress (23); chronic exposure to elevated NEFA was comparable between genotypes, indicating a β-cell–specific protection from lipotoxicity in the MIP-HSD1$^{tg/+}$ mice. In contrast, we find a novel permissive role for 11β-HSD1 in short-term, fatty acid–induced GSIS in vitro, suggesting a physiological role for 11β-HSD1 in meal lipid–related GSIS processes. Further, a direct interaction between GR and PKA has been proposed in other cellular systems (40,44), suggesting a novel mechanism for functional augmentation of β-cells that can now be fully explored. Heat shock protein induction is consistent with increased GR activation (45,46) and, along with p21 in islets (29), is associated with cell survival and protection from apoptosis (28,47), echoing critical processes activated in β-cells that successfully adapt to ER stress (30,45). Note the impact of elevated 11β-HSD1 on β-cell apoptosis will need careful future exploration in model systems other than the HF-fed C57BL/KsJ mice where this process is more evident and quantifiable. Notably, we did not find suppression of inflammatory processes linked to islet damage in type 2 diabetes (48), as occurs when islets are exposed to high levels of corticosterone (45), perhaps reflecting the more physiological nature of β-cell protection in our model. The data therefore give insight into a novel mechanistic framework whereby optimally elevated local glucocorticoid action may facilitate safe execution of increased secretory demand, thus avoiding β-cell failure. Of particular note, given the topical nature of replication as a mechanism for compensation (49,50), the novel protective response of MIP-HSD1$^{tg/+}$ mice does not involve increased β-cell replication. Intriguingly, despite suppressed MIP-HSD1$^{tg/tg}$ islet function under basal (CD) conditions, the markedly elevated β-cell 11β-HSD1 of MIP-HSD1$^{tg/tg}$ elicits an HF diet–responsive β-cell rescue response that is adequate enough to normalize glucose homeostasis. This suggests the potential for mechanistic dissection of therapeutic glucocorticoid effects from those that are undesirable.

Transgenic elevation of β-cell 11β-HSD1 has revealed a novel physiological function for the enzyme in β-cell compensation that may open up new therapeutic opportunities. More broadly, coordinated regulation of local glucocorticoid regeneration in β-cells with dynamic changes in adipose tissue delineates a responsive physiological process that shapes metabolism to protect against metabolic disease. Of more immediate medical significance, our data critically inform imminent therapeutic strategies aimed at manipulation of tissue glucocorticoid action.

ACKNOWLEDGMENTS

These studies were funded by a project grant from Diabetes UK (05/0003083 to N.M.M., J.J.M., and J.R.S.) and supported by a British Heart Foundation Research Excellence Award (BHF REA) (RE/08/001 transition award to S.T. and N.M.M.), a British Endocrine Society Early Career Grant (S.T., N.M., and J.R.S.), a Wellcome Trust Career Development

Fellowship (079660/z/06/z to N.M.M.), and a Wellcome Trust Programme Grant (J.R.S., J.J.M., and B.R.W.). D.R.D. was funded by the Wellcome Trust Cardiovascular Research Initiative and by the BHF REA. Development of the 11β-HSD1 inhibitor UE2316 was supported by a Wellcome Trust Seeding Drug Discovery Award (B.R.W., S.P.W., and J.R.S.).

S.P.W., B.R.W., J.R.S., and N.M.M. hold relevant patents on the use of 11β-HSD1 inhibitors for metabolic indications. No other potential conflicts of interest relevant to this article were reported.

S.T. conceived and designed experiments, researched data, and wrote the manuscript. X.L. and L.R. researched data. S.P.W. and B.R.W. reviewed and edited the manuscript. D.R.D. researched data and reviewed and edited the manuscript. J.J.M. reviewed and edited the manuscript. J.R.S. contributed to discussion and reviewed and edited the manuscript. N.M.M. conceived and designed the experiments, researched data, and wrote the manuscript. N.M.M. is the guarantor of this work and, as such, had full access to all the data in the study and takes responsibility for the integrity of the data and the accuracy of the data analysis.

The authors thank Bernadette Bréant and Amrit Singh-Estivalet (Unité UMRS 872, Paris, France) for helpful advice on islet preparation.

REFERENCES

1. Kahn SE, Hull RL, Utzschneider KM. Mechanisms linking obesity to insulin resistance and type 2 diabetes. Nature 2006;444:840–846
2. Marques AH, Silverman MN, Sternberg EM. Glucocorticoid dysregulations and their clinical correlates. From receptors to therapeutics. Ann N Y Acad Sci 2009;1179:1–18
3. Morton NM, Seckl JR. 11Beta-hydroxysteroid dehydrogenase type 1 and obesity. Front Horm Res 2008;36:146–164
4. Davani B, Khan A, Hult M, et al. Type 1 11beta-hydroxysteroid dehydrogenase mediates glucocorticoid activation and insulin release in pancreatic islets. J Biol Chem 2000;275:34841–34844
5. Duplomb L, Lee Y, Wang MY, et al. Increased expression and activity of 11beta-HSD-1 in diabetic islets and prevention with troglitazone. Biochem Biophys Res Commun 2004;313:594–599
6. Ortsäter H, Alberts P, Warpman U, Engblom LO, Abrahmsén L, Bergsten P. Regulation of 11beta-hydroxysteroid dehydrogenase type 1 and glucose-stimulated insulin secretion in pancreatic islets of Langerhans. Diabetes Metab Res Rev 2005;21:359–366
7. Delaunay F, Khan A, Cintra A, et al. Pancreatic beta cells are important targets for the diabetogenic effects of glucocorticoids. J Clin Invest 1997; 100:2094–2098
8. Lambillotte C, Gilon P, Henquin JC. Direct glucocorticoid inhibition of insulin secretion. An in vitro study of dexamethasone effects in mouse islets. J Clin Invest 1997;99:414–423
9. Hughes KA, Webster SP, Walker BR. 11-Beta-hydroxysteroid dehydrogenase type 1 (11beta-HSD1) inhibitors in type 2 diabetes mellitus and obesity. Expert Opin Investig Drugs 2008;17:481–496
10. Hara M, Wang X, Kawamura T, et al. Transgenic mice with green fluorescent protein-labeled pancreatic beta-cells. Am J Physiol Endocrinol Metab 2003;284:E177–E183
11. Korsgren O, Jansson L, Sandler S, Andersson A. Hyperglycemia-induced B cell toxicity. The fate of pancreatic islets transplanted into diabetic mice is dependent on their genetic background. J Clin Invest 1990;86:2161–2168
12. Morton NM, Paterson JM, Masuzaki H, et al. Novel adipose tissue-mediated resistance to diet-induced visceral obesity in 11 beta-hydroxysteroid dehydrogenase type 1-deficient mice. Diabetes 2004;53:931–938
13. De Sousa Peixoto RA, Turban S, Battle JH, Chapman KE, Seckl JR, Morton NM. Preadipocyte 11beta-hydroxysteroid dehydrogenase type 1 is a ketoreductase and contributes to diet-induced visceral obesity in vivo. Endocrinology 2008;149:1861–1868
14. Alanentalo T, Asayesh A, Morrison H, et al. Tomographic molecular imaging and 3D quantification within adult mouse organs. Nat Methods 2007;4:31–33
15. Wicksteed B, Brissova M, Yan W, et al. Conditional gene targeting in mouse pancreatic β-cells: analysis of ectopic Cre transgene expression in the brain. Diabetes 2010;59:3090–3098
16. Swali A, Walker EA, Lavery GG, Tomlinson JW, Stewart PM. 11Beta-hydroxysteroid dehydrogenase type 1 regulates insulin and glucagon secretion in pancreatic islets. Diabetologia 2008;51:2003–2011
17. Lavery GG, Walker EA, Draper N, et al. Hexose-6-phosphate dehydrogenase knock-out mice lack 11 beta-hydroxysteroid dehydrogenase type 1-mediated glucocorticoid generation. J Biol Chem 2006;281:6546–6551
18. Butler AE, Janson J, Bonner-Weir S, Ritzel R, Rizza RA, Butler PC. Beta-cell deficit and increased beta-cell apoptosis in humans with type 2 diabetes. Diabetes 2003;52:102–110
19. Bernardo AS, Hay CW, Docherty K. Pancreatic transcription factors and their role in the birth, life and survival of the pancreatic beta cell. Mol Cell Endocrinol 2008;294:1–9
20. Bréant B, Gesina E, Blondeau B. Nutrition, glucocorticoids and pancreas development. Horm Res 2006;65(Suppl. 3):98–104
21. Gao Z, Young RA, Trucco MM, et al. Protein kinase A translocation and insulin secretion in pancreatic beta-cells: studies with adenylate cyclase toxin from *Bordetella pertussis*. Biochem J 2002;368:397–404
22. Lawrence JT, Birnbaum MJ. ADP-ribosylation factor 6 regulates insulin secretion through plasma membrane phosphatidylinositol 4,5-bisphosphate. Proc Natl Acad Sci USA 2003;100:13320–13325
23. Yusta B, Baggio LL, Estall JL, et al. GLP-1 receptor activation improves beta cell function and survival following induction of endoplasmic reticulum stress. Cell Metab 2006;4:391–406
24. Cram EJ, Ramos RA, Wang EC, Cha HH, Nishio Y, Firestone GL. Role of the CCAAT/enhancer binding protein-alpha transcription factor in the glucocorticoid stimulation of p21waf1/cip1 gene promoter activity in growth-arrested rat hepatoma cells. J Biol Chem 1998;273:2008–2014
25. Ehses JA, Pelech SL, Pederson RA, McIntosh CH. Glucose-dependent insulinotropic polypeptide activates the Raf-Mek1/2-ERK1/2 module via a cyclic AMP/cAMP-dependent protein kinase/Rap1-mediated pathway. J Biol Chem 2002;277:37088–37097
26. Eum WS, Li MZ, Sin GS, et al. Dexamethasone-induced differentiation of pancreatic AR42J cell involves p21(waf1/cip1) and MAP kinase pathway. Exp Mol Med 2003;35:379–384
27. Ramalingam A, Hirai A, Thompson EA. Glucocorticoid inhibition of fibroblast proliferation and regulation of the cyclin kinase inhibitor p21Cip1. Mol Endocrinol 1997;11:577–586
28. Wang J, Devgan V, Corrado M, et al. Glucocorticoid-induced tumor necrosis factor receptor is a p21Cip1/WAF1 transcriptional target conferring resistance of keratinocytes to UV light-induced apoptosis. J Biol Chem 2005;280:37725–37731
29. Burkhardt BR, Greene SR, White P, et al. PANDER-induced cell-death genetic networks in islets reveal central role for caspase-3 and cyclin-dependent kinase inhibitor 1A (p21). Gene 2006;369:134–141
30. D'Hertog W, Maris M, Ferreira GB, et al. Novel insights into the global proteome responses of insulin-producing INS-1E cells to different degrees of endoplasmic reticulum stress. J Proteome Res 2010;9:5142–5152
31. Du J, Wang Y, Hunter R, et al. Dynamic regulation of mitochondrial function by glucocorticoids. Proc Natl Acad Sci USA 2009;106:3543–3548
32. Kjørholt C, Akerfeldt MC, Biden TJ, Laybutt DR. Chronic hyperglycemia, independent of plasma lipid levels, is sufficient for the loss of beta-cell differentiation and secretory function in the db/db mouse model of diabetes. Diabetes 2005;54:2755–2763
33. Holness MJ, Smith ND, Greenwood GK, Sugden MC. Interactive influences of peroxisome proliferator-activated receptor alpha activation and glucocorticoids on pancreatic beta cell compensation in insulin resistance induced by dietary saturated fat in the rat. Diabetologia 2005;48:2062–2068
34. Ogawa A, Johnson JH, Ohneda M, et al. Roles of insulin resistance and beta-cell dysfunction in dexamethasone-induced diabetes. J Clin Invest 1992;90:497–504
35. Rafacho A, Marroquí L, Taboga SR. Glucocorticoids in vivo induce both insulin hypersecretion and enhanced glucose sensitivity of stimulus-secretion coupling in isolated rat islets. Endocrinology 2010;151:85–95
36. Koizumi M, Yada T. Sub-chronic stimulation of glucocorticoid receptor impairs and mineralocorticoid receptor protects cytosolic Ca2+ responses to glucose in pancreatic beta-cells. J Endocrinol 2008;197:221–229
37. Reinbothe TM, Ivarsson R, Li DQ, et al. Glutaredoxin-1 mediates NADPH-dependent stimulation of calcium-dependent insulin secretion. Mol Endocrinol 2009;23:893–900
38. Löwenberg M, Tuynman J, Scheffer M, et al. Kinome analysis reveals nongenomic glucocorticoid receptor-dependent inhibition of insulin signaling. Endocrinology 2006;147:3555–3562
39. Hult M, Elleby B, Shafqat N, et al. Human and rodent type 1 11beta-hydroxysteroid dehydrogenases are 7beta-hydroxycholesterol dehydrogenases involved in oxysterol metabolism. Cell Mol Life Sci 2004;61: 992–999

40. Doucas V, Shi Y, Miyamoto S, West A, Verma I, Evans RM. Cytoplasmic catalytic subunit of protein kinase A mediates cross-repression by NF-kappa B and the glucocorticoid receptor. Proc Natl Acad Sci USA 2000;97:11893–11898
41. Efanov AM, Sewing S, Bokvist K, Gromada J. Liver X receptor activation stimulates insulin secretion via modulation of glucose and lipid metabolism in pancreatic beta-cells. Diabetes 2004;53(Suppl. 3):S75–S78
42. Cha HH, Cram EJ, Wang EC, Huang AJ, Kasler HG, Firestone GL. Glucocorticoids stimulate p21 gene expression by targeting multiple transcriptional elements within a steroid responsive region of the p21waf1/cip1 promoter in rat hepatoma cells. J Biol Chem 1998;273:1998–2007
43. Trümper J, Ross D, Jahr H, Brendel MD, Göke R, Hörsch D. The Rap-B-Raf signalling pathway is activated by glucose and glucagon-like peptide-1 in human islet cells. Diabetologia 2005;48:1534–1540
44. Louiset E, Stratakis CA, Perraudin V, et al. The paradoxical increase in cortisol secretion induced by dexamethasone in primary pigmented nodular adrenocortical disease involves a glucocorticoid receptor-mediated effect of dexamethasone on protein kinase A catalytic subunits. J Clin Endocrinol Metab 2009;94:2406–2413
45. Hult M, Ortsäter H, Schuster G, et al. Short-term glucocorticoid treatment increases insulin secretion in islets derived from lean mice through multiple pathways and mechanisms. Mol Cell Endocrinol 2009; 301:109–116
46. Grad I, Picard D. The glucocorticoid responses are shaped by molecular chaperones. Mol Cell Endocrinol 2007;275:2–12
47. Harms C, Albrecht K, Harms U, et al. Phosphatidylinositol 3-Akt-kinase-dependent phosphorylation of p21(Waf1/Cip1) as a novel mechanism of neuroprotection by glucocorticoids. J Neurosci 2007;27:4562–4571
48. Donath MY, Böni-Schnetzler M, Ellingsgaard H, Ehses JA. Islet inflammation impairs the pancreatic beta-cell in type 2 diabetes. Physiology (Bethesda) 2009;24:325–331
49. Liu Y, Mziaut H, Ivanova A, Solimena M. Beta-cells at the crossroads: choosing between insulin granule production and proliferation. Diabetes Obes Metab 2009;11(Suppl. 4):54–64
50. Sachdeva MM, Stoffers DA. Minireview: meeting the demand for insulin: molecular mechanisms of adaptive postnatal beta-cell mass expansion. Mol Endocrinol 2009;23:747–758